Ramshaw, J. A. M. (1982) *Encycl. Plant Physiol., New Ser. 14A*, 229-240.
Ramshaw, J. A. M., Brown, R. H., Scawen, M. D., & Boulter, D. (1973) *Biochim. Biophys. Acta 303*, 269-273.
Rance, M., & Wright, P. E. (1986) *J. Magn. Reson. 66*, 372-378.
Redfield, C., Hoch, J. C., & Dobson, C. M. (1983) *FEBS Lett. 159*, 132-136.
Ulrich, E. L., & Markley, J. L. (1978) *Coord. Chem. Rev. 27*, 109-140.
Wagner, G., & Wüthrich, K. (1982) *J. Mol. Biol. 155*, 347-366.
Wagner, G., Kumar, A., & Wüthrich, K. (1981) *Eur. J. Biochem. 114*, 375-384.
Wüthrich, K., Wider, G., Wagner, G., & Braun, W. (1982) *J. Mol. Biol. 155*, 311-319.

Resonance Raman Studies of Isotopically Labeled Chloroperoxidase†

O. Bangcharoenpaurpong and P. M. Champion*
Department of Physics, Northeastern University, Boston, Massachusetts 02115
K. S. Hall and L. P. Hager
Department of Biochemistry, University of Illinois, Urbana, Illinois 61801
Received October 7, 1985; Revised Manuscript Received January 13, 1986

ABSTRACT: Chloroperoxidase (CPO) and cytochrome $P450_{cam}$ have been shown by several techniques to have similar active site properties. Recent resonance Raman investigations using isotopically enriched ^{34}S-labeled samples have demonstrated thiolate ligation in the $P450_{cam}$ system. We report here on a number of parallel studies involving CPO. On the basis of isotopic labeling (^{34}S, ^{13}CO), we assign the Fe–S and Fe–CO stretching frequencies of CPO at 347 ($\bar{\nu}_{Fe-S}$) and 488 cm^{-1} ($\bar{\nu}_{Fe-CO}$). The differences of the $\bar{\nu}_{Fe-S}$ and $\bar{\nu}_{Fe-CO}$ in CPO and $P450_{cam}$ may suggest subtle differences in the thiolate binding in the two systems.

Chloroperoxidase (CPO) is a heme protein of M_r ~42 000 which has been isolated from the mold *Caldariomyces fumago* (Morris & Hager, 1966). It catalyzes the chlorination reactions involved in the biosynthesis of caldariomycin (2,2-dichloro-1,3-cyclopentanedione). In the presence of hydrogen peroxide and a suitable halogen donor (I^-, Br^-, or Cl^-, but not F^-), the enzyme catalyzes the peroxidative formation of a carbon–halogen bond with a suitable halogen acceptor. In addition to the halogenation reaction, chloroperoxidase also catalyzes the peroxidative oxidation of classical peroxidase substrates such as pyrogallol and guaiacol (Thomas et al., 1970), and it catalyzes the decomposition of hydrogen peroxide to give molecular oxygen in a catalase type reaction.

Previous resonance Raman studies of chloroperoxidase have focused primarily on the high-frequency "marker band" region of the spectrum that involves the porphyrin ring stretching modes (Champion et al., 1976; Remba et al., 1979). The relatively low value found for the frequency of the ring-breathing mode (oxidation state marker), ν_4, in CPO is thought to reflect an electron-rich axial ligand that donates electron density into the porphyrin π^* anti-bonding orbitals (Champion et al., 1976; 1978; Remba et al., 1979; Ozaki et al., 1978). Comparisons between the resonance Raman spectra of CPO and cytochrome $P450_{cam}$ have also been stressed in an earlier work (Remba et al., 1979) and are thought to reflect a high degree of similarity in the active sites of these two very different heme proteins. In this respect, the Raman observations are consistent with a variety of other physical–chemical studies including Mössbauer (Champion et al., 1973, 1975), optical (Hollenberg & Hager, 1973), electron spin resonance (Hollenberg et al., 1980), magnetic circular dichroism (Dawson et al., 1983), and extended X-ray fine structure (Cramer et al., 1978) in that they suggest that both proteins utilize the electron-rich mercaptide sulfur of cysteine as the axial ligand to the heme iron.

Recent resonance Raman investigations (Champion et al., 1982) of cytochrome $P450_{cam}$ enriched in ^{34}S and ^{54}Fe have conclusively demonstrated that cytochrome $P450_{cam}$ does indeed possess an Fe–S linkage, and the Fe–S stretching frequency is found at 351 cm^{-1}. The resonance enhancement of the Fe–S mode in $P450_{cam}$ is presumably due to a S → Fe charge-transfer transition underlying the intense Soret band. This is evidenced by the fact that the Raman excitation profile of the 351-cm^{-1} mode peaks nearly 1500 cm^{-1} to the blue of the Soret maximum. (If this mode were coupled to the Soret resonance, it would be expected to peak within ca. 350 cm^{-1} of the Soret maximum.) In addition, the magnitude of the isotopic shifts in the $P450_{cam}$ system are suggestive of a more open Fe–S–C bond angle than would normally be expected for sp^3 sulfur bonding. One possible explanation for this observation is that the sulfur bonding involves an sp^2 hybrid geometry in the P450 system, with the remaining p orbital interacting through a coordinate covalent π-bonding arrangement with one of the $d\pi$ orbitals of iron (Champion et al., 1982). This type of bonding geometry could also explain the highly rhombic electron paramagnetic resonance (EPR) splittings found for the P450 class of heme proteins (Hollenberg et al., 1980; Chevion et al., 1977).

As a result of the success in the definitive assignment of the sulfur ligand in the $P450_{cam}$ system, we decided to investigate isotopically labeled CPO in order to confirm the expected Fe–S linkage and possibly gain additional information about the Fe–S–C bonding geometry. We report below the results of

† This work is supported by grants from the National Institutes of Health (AM35090), The Research Corporation, and the National Science Foundation. P.M.C. is a recipient of NIH Research Center Career Development Award AM01405.

0006-2960/86/0425-2374$01.50/0 © 1986 American Chemical Society

our studies on the CPO system using ^{34}S and ^{13}CO as well as some parallel studies of $P450_{cam}$ in the oxidized (m^o) and substrate bound (m^{os}) forms.

Experimental Procedures

The chloroperoxidase (CPO) samples, enriched in ^{34}S, are isolated from *Caldariomyces fumago* grown on a chemically defined media with $H_2{}^{34}SO_4$ as the sole source of sulfur. The amount of ^{34}S incorporated into purified CPO (Morris & Hager, 1966) ($R_z > 1.4$) is determined by gas chromatography–mass spectroscopy (GC–MS) (chemical ionization). Purified CPO is hydrolyzed with 6 N HCl at 150 °C for 1 h. After hydrolysis the resulting amino acids are converted into their *N*-trifluoroacetyl *n*-butyl ester (TAB) derivatives (Darbre, 1978). Separation of the TAB-amino acids is carried out on a DB-5, 30-m capillary column using an initial temperature of 60 °C with a 4 °C/min program. The excess atom percent ^{34}S of TAB-Met is determined by the same procedure described by White (White, 1981). The total incorporation, including natural abundance ^{34}S, is found to be 96.4 ± 1% in the ^{34}S-labeled chloroperoxidase sample.

A Raman sample of CPO is prepared by dilution of the concentrated CPO solution with the 150 mM potassium phosphate buffer, pH 3.0, to a desired concentration of about 70 μM. The sample is then characterized before and after the scattering experiment using a Perkin-Elmer 320 UV–VIS spectrophotometer.

The CPO–CO complex is prepared by transferring the CPO solution into a glass cylinder cuvette with a serum cap on the top. The solution is slowly bubbled with ^{12}CO or ^{13}CO (Cambridge Isotope, Cambridge, MA) gas for ca. 30 min and then transferred into another cylindrical cuvette which contains sodium dithionite and ^{12}CO or ^{13}CO gas. The CO complex is characterized by optical absorption and used immediately.

The Raman spectra are accumulated by using a Spex 1403 double monochromator, a cooled RCA 31034 phototube, and photon counting electronics (Princeton Applied Research). The excitation source is a Spectra Physics 171 argon ion laser that is used individually (363.8 nm) or in conjunction with a Coherent 599 dye laser. Both the Raman and the UV–vis spectrophotometers are interfaced to a DEC Minc 11/23 based laboratory computer system. The samples are kept at 15 °C during the scattering experiments using a thermoelectric cooler. A 90° scattering geometry is employed, and a spinning cell arrangement at room temperature is used for the photolabile CO complex. All Raman spectra are accumulated in a sequential scan mode, with a resulting accuracy that is determined by monochromator backlash. Use of the 981-cm^{-1} band of sulfate as an internal intensity standard also serves as a frequency calibration. Numerous repetitive scans using standard samples have convinced us that our absolute frequency error is in the ±1-cm^{-1} range using this technique. The relative errors are much smaller.

Results

In Figure 1 we display the Soret absorption bands of native CPO and two forms of cytochrome $P450_{cam}$. The laser excitation frequencies used in this study are also shown. We recall here that the substrate-bound form of cytochrome $P450_{cam}$ (m^{os}) is known to have the heme iron atom in the high-spin ferric state, while the substrate free form (m^o) has a low-spin ferric iron atom (Gunsalus et al., 1974). The optical absorption bands reflect this spin-state change dramatically as do the Raman spectra (Champion et al., 1978).

Native chloroperoxidase, on the other hand, has an absorption band that may reflect a spin mixture, even at room temperature. It is known from low-temperature Mössbauer and EPR studies that CPO undergoes a temperature-dependent spin transition that favors the high-spin form at higher temperatures (Champion et al., 1975). Analysis of the CPO Raman spectra also suggests a dominant high-spin fraction at room temperature (Remba et al., 1979).

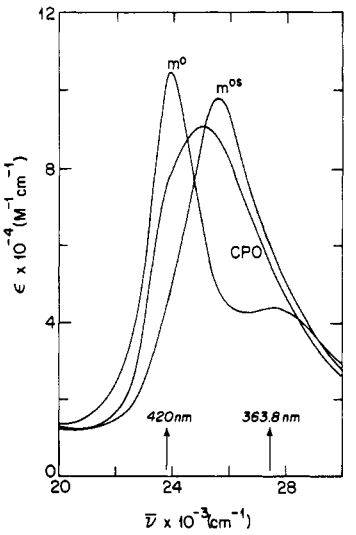

FIGURE 1: Absorption spectra of m^o, m^{os}, and CPO. The arrows indicate the excitation frequencies used in the resonance Raman experiments.

Table I: Low-Frequency Raman Spectra of Native CPO

	$\bar{\nu}_L{}^a$ = 23809 cm^{-1} (420 nm)		$\bar{\nu}_L$ = 27487 cm^{-1} (363.8 nm)		
protein	$\Delta\bar{\nu}$ (cm^{-1})	$(d\sigma/d\Omega)^b \times 10^{25}$	$\Delta\bar{\nu}$ (cm^{-1})	$(d\sigma/d\Omega) \times 10^{25}$	R^c
CPO	262	1.30[d]	262	0.17	0.13
	348	2.92[d]	347	0.71	0.24
	377	1.16[d]	380	0.16	0.14
	417	2.04[d]	417	0.33	0.16
m^{os}	345	0.36			0
			351	1.36	∞
	377	0.49	377	0.17	0.35
	422	0.19			0
m^o	345	6.77			0
	379	5.97			0
	426	5.17			0

[a] $\bar{\nu}_L$ is laser excitation frequency [$\bar{\nu}_L$ is 23 980 cm^{-1} (417 nm) for the m^o complex]. [b] Differential cross section ($I_\parallel + I_\perp$) in cm^2/(steradian·molecule). [c] R is the ratio of the scattering cross section at 363.8 nm to that at 420 nm. [d] The concentrations used for determination of the cross sections do not account for the fact that low-spin and high-spin mixtures are present in the samples. For example, if the low-frequency modes are associated only with the low-spin fraction, the cross sections should be scaled up by this fraction and might be expected to be on the order of those found for the m^o complex. It may also be noted that the weak low-frequency peaks in m^{os}, excited at 420 nm, could be accounted for by the presence of ca. 5–10% low-spin material.

In Table I we delineate the low-frequency Raman spectra of native CPO. The mode frequencies and the absolute cross sections are summarized along with the analogous modes of cytochrome $P450_{cam}$. As the laser is tuned from 420.0 to 363.8 nm, no major new bands become obviously apparent in the CPO spectra. This behavior stands in marked contrast to the differential resonance enhancement of the 351-cm^{-1} mode in the (363.8-nm) m^{os} Raman spectrum. It appears, at first, that the low-frequency modes of CPO are coupled to the Soret resonance and are simply dropping off in intensity as the laser is tuned into the ultraviolet. (These modes may be due to the low-spin material which will show maximum resonance en-

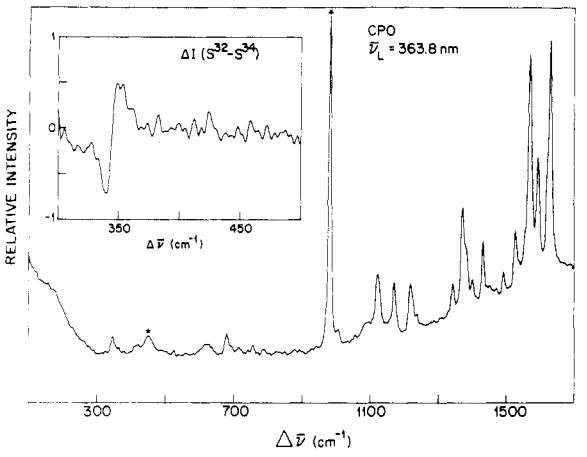

FIGURE 2: Resonance Raman spectrum of CPO excited at 363.8 nm. The concentration of CPO is 75 μM in 1.0 M $(NH_4)_2SO_4$ and 150 mM potassium phosphate buffer. The experimental conditions were 3-cm^{-1} resolution, 2-cm^{-1} step size, 10-s count time, and ca. 20 mW at the sample. The sulfate vibrations at 450 and 981 cm^{-1} are indicated by asterisks. The insert shows the Raman difference spectrum of a separate experiment using native (^{32}S) and ^{34}S-enriched CPO without sulfate added. These spectra were run sequentially with 1-cm^{-1} step size and 3-cm^{-1} resolution. The spectra were smoothed by using standard techniques and the ^{34}S-enriched spectrum was normalized to the area of the corresponding native spectrum followed by background subtraction. The difference is then obtained as discussed previously (Champion et al., 1982).

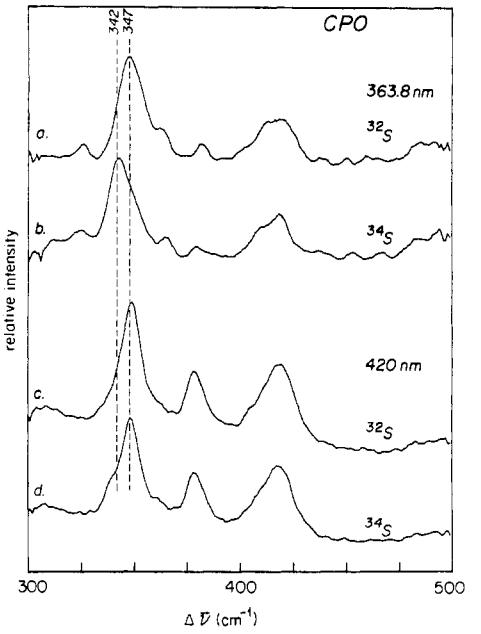

FIGURE 3: Resonance Raman spectra of native (a) and ^{34}S-enriched (b) CPO excited at 363.8 nm (top) and at 420 nm (bottom, curves c and d). Experimental conditions were the same as in Figure 2 except for 1-cm^{-1} step size and 2-cm^{-1} resolution at 420-nm excitation.

hancement at ca. 420.0 nm.) Note that, the the exception of the 347–348-cm^{-1} mode, the Raman intensities at 363.8 nm are reduced with respect to excitation at 420.0 nm by a factor of ca. 7. It turns out (vide infra) that the Fe–S mode of CPO is less strongly enhanced than in $P450_{cam}$ and accidentally degenerate with another mode in the 345–350-cm^{-1} region. This accounts for the increase in *relative* intensity of the 347–348-cm^{-1} mode by using 363.8-nm excitation.

In order to test for the presence of the suspected Fe–S vibration, we measured the low-frequency Raman spectrum of the native and ^{34}S-enriched CPO samples using laser excitation at both 363.8 and 420.0 nm. The Raman difference spectrum (^{32}S–^{34}S) obtained at 363.8 nm is displayed in Figure 2 and definitely indicates the presence of an Fe–S bond in the CPO system. The fact that the other low-frequency modes at 380 and 417 cm^{-1} give an essentially perfect null in the difference spectrum allows us to conclusively assign the 347-cm^{-1} mode to the Fe–S vibration in CPO. The overall isotopic shift of this mode is calculated by previous methods (Champion et al., 1982) and is found to be $\Delta_S = -4.9 \pm 0.5$ cm^{-1}. We also carefully investigated the 625–825-cm^{-1} region of the spectrum in an attempt to identify the Fe–S overtone; however, no shifts were observed, and the overtone assignment could not be made.

In Figure 3 we have displayed the actual Raman line shapes for native and ^{34}S-labeled CPO using laser excitation at 363.8 and 420.0 nm. It is clear that at least two vibrational modes are present in the 340–350-cm^{-1} region. This is most obvious in the ^{34}S spectrum taken at 420.0 nm (curve d). When the laser frequency is shifted to 363.8 nm, the low-frequency modes coupled to the π–π^* Soret transition show a decrease in scattering cross section as can be seen in Table I. On the other hand, the Fe–S mode at 347 cm^{-1}, which may be coupled to an out of plane S → Fe charge-transfer transition, shows an increase in intensity upon 363.8-nm excitation. This increase is less pronounced in the case of CPO than it is for the 351-cm^{-1} mode of the m^{os} form of cytochrome P450 (see Table I) but is nevertheless easily discernible. The isotopic shift of the

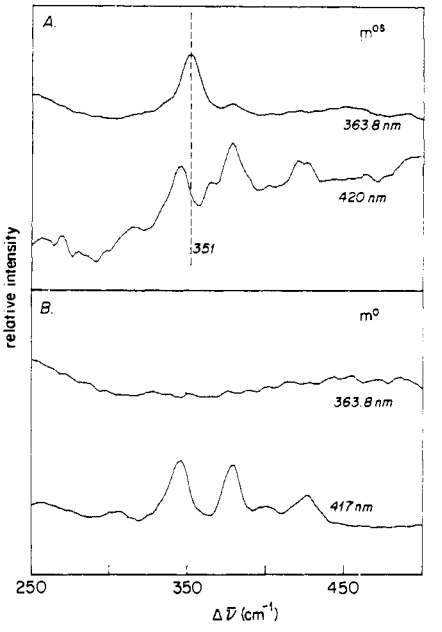

FIGURE 4: Resonance Raman spectra of (A) m^{os} excited at 363.8 (top, 4-cm^{-1} resolution) and 420 nm (bottom, 5-cm^{-1} resolution) and (B) m^{o} excited at 363.8 (top, 4-cm^{-1} resolution) and 417 nm (bottom, 3-cm^{-1} resolution). In all samples the 0.5 M $(NH_4)_2SO_4$ is added as an internal standard.

347-cm^{-1} mode is therefore calculated by using spectra taken at 363.8 nm where there is less contribution from the interfering π–π^* coupled low-frequency mode. Using Table I as a guide, we expect that, at 363.8 nm, <50% of the intensity in the 340–350-cm^{-1} region of the CPO spectrum can be attributed to the π–π^* coupled mode at 348 cm^{-1}.

In order to emphasize the differences between these results and those found for the $P450_{cam}$ system, we display in Figure 4A the low-frequency Raman spectra of cytochrome $P450_{cam}$ (m^{os}) taken at 420.0- and 363.8-nm laser excitation. The frequencies and cross sections of the P450 modes are found in Table I. Note that the Fe–S mode at 351 cm^{-1} is clearly enhanced independently of the other low-frequency modes and

Table II: Fe–CO Vibrational Frequencies of Various Heme Proteins and Model Compounds

protein[a] and model compound	$\bar{\nu}$ (cm^{-1}) $\bar{\nu}_{Fe-CO}$	δ_{Fe-CO}	technique	reference
Protein				
cytochrome oxidase	520	578	$^{13}C^{16}O$	Argade et al. (1984)
Mb	512	577	$^{13}C^{16}O$, $^{12}C^{18}O$	Tsubaki et al. (1982)
Hb	507	578	$^{13}C^{18}O$	Tsubaki et al. (1982)
LHb	505		$^{13}C^{18}O$	Armstrong et al. (1982)
CPO	488		$^{13}C^{16}O$	this work
$P450_{cam}$ (m^{os})	481	558	$^{13}C^{16}O$, $^{12}C^{18}O$	Uno et al. (1985)
$P450_{scc}$	477		$^{12}C^{18}O$	Tsubaki & Ichikawa (1985)
$P450_{LM}$	474		$^{13}C^{16}O$	Anzenbacher et al. (1985)
$P450_{cam}$ (m^{o})	464–469	556	$^{12}C^{18}O$	Uno et al. (1985); Champion (1986)
Model Compound				
$Fe(T_{piv})(THF)(CO)$ strapped hemes	526		$^{13}C^{16}O$, $^{12}C^{18}O$, $^{13}C^{18}O$	Kerr et al. (1983)
FeSP-13	514		$^{13}C^{16}O$	Yu et al. (1983)
FeSP-14	512		$^{13}C^{16}O$, $^{12}C^{18}O$, $^{13}C^{18}O$	Yu et al. (1983)
FeSP-15	509		$^{13}C^{16}O$	Yu et al. (1983)
Fe(heme 5)(*N*-MeIm)(CO) (unstrapped)	495		$^{13}C^{16}O$, $^{12}C^{18}O$, $^{13}C^{18}O$	Yu et al. (1983)
$Fe(T_{piv}PP)$(*N*-MeIm)(CO)	489		$^{13}C^{16}O$, $^{12}C^{18}O$, $^{13}C^{18}O$	Kerr et al. (1983)
$Fe(T_{piv}PP)(PY)(CO)$	486		$^{13}C^{16}O$, $^{12}C^{18}O$, $^{13}C^{18}O$	Kerr et al. (1983)
$Fe(T_{piv}PP)(C_6HF_4S)(CO)$	479		$^{13}C^{16}O$	Chottard et al. (1984)

[a] Abbreviations: $P450_{LM}$, cytochrome P-450 from liver microsome; $P450_{scc}$, cytochrome P-450 from adrenal cortex mitochondria; Mb, myoglobin; Hb, hemoglobin; CPO, chloroperoxidase; LHb, leghemoglobin; PY, pyridine; *N*-MeIm, 1-methylimidazole.

is only observed upon 363.8 nm excitation when the other modes have almost completely disappeared. This enhancement pattern is somewhat different from the one displayed by chloroperoxidase which does not show such strong evidence for a separately enhanced low-frequency mode due to the almost perfect overlap of mode frequencies at 347 and 348 cm^{-1}.

It is also of interest to compare the low-frequency resonance enhancement pattern of CPO and m^{os} to that of the oxidized, low-spin native $P450_{cam}$ complex (m^{o}). Figure 4B shows the spectra taken at 363.8 and 417.0 nm, while Table I lists the cross sections and frequencies of the m^{o} complex. The cross sections are greatly enhanced at 417.0 nm due to the fact that the laser is in direct resonance with the Soret transition of m^{o}. Notice that no low-frequency modes are observed at 363.8-nm excitation, suggesting that the charge-transfer resonance which is presumably responsible for the enhancement of the 351 cm^{-1} mode in m^{os} is substantially altered when the heme system switches from the high-spin to the low-spin configuration. This result emphasizes how variations in the local electronic structure of the heme can profoundly affect the resonance enhancement pattern of the low-frequency modes.

In Figure 5 we display resonance Raman spectra of carbon monoxide bound CPO. In this state the Soret band is found near 450 nm and is indicative of a P450 type heme protein (Champion et al., 1973; Hollenberg & Hager, 1973). Experiments with ^{13}CO allow us to assign the Fe–CO stretching vibration to the mode at 488 cm^{-1} although the precise magnitude of the isotopic shift is difficult to quantify due to the breadth and asymmetry of the Raman line shape. The nonuniform line shape may be due to sample inhomogeneity brought about by the general instability of the reduced CPO complex. It must be noted that CPO belongs to the peroxidase class of heme proteins and prefers higher oxidation states of the heme iron. Cytochrome P450, on the other hand, has a naturally occurring Fe^{2+} state.

Discussion

In Table II we have summarized some of the recent results involving the Fe–CO vibrations of various heme proteins and model compounds. It should be noted that, in general, a depressed Fe–CO frequency results when an electron-rich

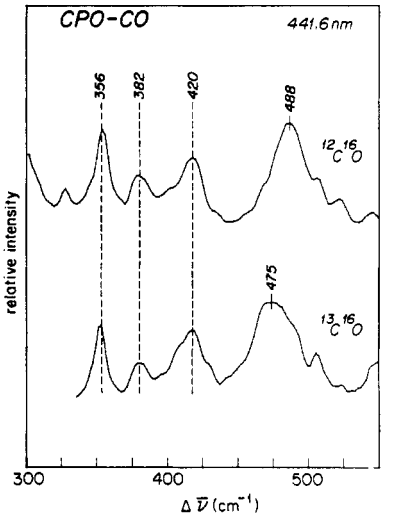

FIGURE 5: Resonance Raman spectra of the CPO–CO complex (top) and CPO–^{13}CO complex (bottom). The excitation energy was 442 nm, and the resolution was 3 cm^{-1}. Power at the sample was about 10 mW and 1.0 M $(NH_4)_2SO_4$ was an internal standard.

sulfur ligand is bound trans to the Fe–CO linkage. It is particularly interesting that absence of the camphor substrate in the $P450_{cam}$ system results in an extremely low Fe–CO frequency (464–469 cm^{-1}) while its presence results in a frequency (481 cm^{-1}) more similar to that of CPO–CO (488 cm^{-1}). This effect has been tentatively explained (Uno et al., 1985) by analogy with strapped heme complexes (see Table II) with the implication that camphor strains the Fe–CO bond. [Under certain circumstances it is evidently possible to increase the Fe–CO frequency when steric constraints are applied to the Fe–CO bond (Yu et al., 1983).] Nevertheless, we find it somewhat perplexing that both CPO–CO and the picket fence model compound, $Fe(T_{piv}PP)(C_6HF_4S)(CO)$, have Fe–CO frequencies in the 480–490-cm^{-1} range and presumably do not have significant steric hindrance of the Fe–CO bond due to bound substrate. Further work is in progress in order to better understand these effects.

The frequency of the Fe–S mode of CPO is also somewhat different than found for the m^{os} form of $P450_{cam}$. It may turn out that subtle differences in the sulfur → iron electron do-

nation in the two systems is reflected in both the Fe–S and the Fe–CO frequencies. The higher Fe–CO frequency found for CPO (488 cm^{-1}) vs. that for P450 (481 cm^{-1}) indicates a stronger Fe–CO bond for CPO and may be related to the weaker Fe–S linkage in CPO ($\bar{\nu}_{Fe-S}$ = 347 cm^{-1}) compared to that in $P450_{cam}$ ($\bar{\nu}_{Fe-S}$ = 351 cm^{-1}). Various interpretations of the Fe–CO frequencies of P450 have been discussed and have involved conformational strain (Uno et al., 1985), π-back-bonding effects (Tsubaki & Ishikawa, 1985), and σ-bonding properties (Chottard et al., 1984) of the iron ligand system. We feel that care must be exercised in such interpretations because all three effects may be operative and combine together to yield the observed Fe–CO frequency. (For example, the S → Fe ← CO σ donation and the Fe → CO π-back-bonding effects are probably intricately connected.) Related effects are observed in the Raman spectrum of the oxygenated complex of $P450_{cam}$ where thiolate electron donation into the π^*_g orbitals of oxygen causes a substantial downshift of the dioxygen stretching frequency to 1140 cm^{-1} (Bangcharoenpaurpong et al., 1986).

The identification of the Fe–S vibration of CPO at 347 cm^{-1} along with its −4.9 cm^{-1} downshift upon ^{34}S substitution provides definite evidence that CPO has a sulfur ligand that is nearly identical with that of cytochrome $P450_{cam}$. This ligand is almost certainly the mercaptide sulfur of cysteine, and given the coincidence of isotopic shifts (Δ_S^{P450} = −4.9 cm^{-1}), we suggest that the iron–sulfur bonding geometry is basically the same in CPO ad $P450_{cam}$. The details of the bonding in both systems (e.g., bond angles, hybridization of sulfur, etc.) must await the results of high-resolution X-ray crystallography.

In summary, we report the definite assignment of the Fe–S vibrational mode in CPO (347 cm^{-1}) as well as the Fe–CO mode (488 cm^{-1}) in the carbon monoxide complex. The available evidence points strongly to nearly equivalent active sites in CPO and $P450_{cam}$. However, there appears to be subtle and possibly systematic differences in the iron ligand bonding strengths as reflected by the Fe–S and Fe–CO vibrational frequencies. Further work involving the variation of resonance Raman intensities with laser excitation frequency is currently in progress. The preliminary evidence using "inverse transform" techniques (Bangcharoenpaurpong et al., 1984; Lee et al., 1985; Champion, 1986) suggests that the electronic transitions responsible for the Fe–S resonance enhancement may be somewhat different in CPO and $P450_{cam}$.

ACKNOWLEDGMENTS

We thank Dr. G. C. Wagner for preparation of the $P450_{cam}$ samples.

REFERENCES

Anzenbacher, P., Fidler, V., Schenkman, J. B., Kirkup, R. E., & Spiro, T. G. (1985) *Biochim. Biophys. Acta 827*, 474.

Argade, D. V., Ching, Y. C., & Rousseau, D. L. (1984) *Science (Washington, D.C.) 225*, 329.

Armstrong, R. S., Irwin, M. J., & Wright, P. E. (1982) *J. Am. Chem. Soc. 104*, 626.

Bangcharoenpaurpong, O., Schomacker, K. T., & Champion, P. M. (1984) *J. Am. Chem. Soc. 106*, 5688.

Bangcharoenpaurpong, O., Rizos, A. K., Champion, P. M., Jollie, D., & Sligar, S. G. (1986) *J. Biol. Chem.* (submitted for publication).

Champion, P. M. (1986) in *Biological Applications of Raman Spectroscopy* (Spiro, T. G., Ed.) Wiley, New York (in press).

Champion, P. M., Munck, E., Debrunner, P., Hollenberg, P., & Hager, L. P. (1973) *Biochemistry 12*, 426.

Champion, P. M., Chang, R., Munck, E., Debrunner, P., & Hager, L. P. (1975) *Biochemistry 14*, 4159.

Champion, P. M., Remba, R., Chiang, R., Fitchen, D. B., & Hager, L. P. (1976) *Biochim. Biophys. Acta 446*, 486.

Champion, P. M., Gunsalus, I. C., & Wagner, G. C. (1978) *J. Am. Chem. Soc. 100*, 3743.

Champion, P. M., Stallard, B. R., Wagner, G. C., & Gunsalus, I. C. (1982) *J. Am. Chem. Soc. 104*, 5469.

Chevion, M., Peisach, J., & Blumberg, W. E. (1977) *J. Biol. Chem. 252*, 3637.

Chottard, G., Schappacher, M. Ricard, L., & Weiss, R. (1984) *Inorg. Chem. 23*, 4557.

Cramer, S. P., Dawson, J. H., Hodgson, K., & Hager, L. P. (1978) *J. Am. Chem. Soc. 100*, 7282.

Darbre, A. (1978) in *Handbook of Derivatives for Chromatography* (King, G. S., & Blau, K., Eds.) p 67, Heyden and Sons, Philadelphia, PA.

Dawson, J. H., Sono, M., & Hager, L. P. (1983) *Inorg. Chim. Acta 79*, 184.

Gunsalus, I. C., Meeks, J. R., Lipscomb, J. D., Debrunner, P., & Munck, E. (1974) in *Molecular Mechanisms of Oxygen Activation* (Hayaishi, O., Ed.) p 559, Academic, New York.

Hollenberg, P. F., & Hager, L. P. (1973) *J. Biol. Chem. 248*, 2630.

Hollenberg, P. F., Hager, L. P., Blumberg, W. E., & Peisach, J. (1980) *J. Biol. Chem. 255*, 4801.

Kerr, E. A., Mackin, H. C., & Yu, N. T. (1983) *Biochemistry 22*, 4373.

Lee, D. H., Stallard, B., Champion, P. M., & Albrecht, A. C. (1985) *J. Phys. Chem. 88*, 6693.

Morris, D. R., & Hager, L. P. (1966) *J. Biol. Chem. 241*, 1763.

Ozaki, Y., Kitagawa, T., Kyogoku, Y., Imai, Y., Yutsudo, C., & Sato, R. (1978) *Biochemistry 17*, 5826.

Remba, R., Champion, P. M., Fitchen, D. B., Chiang, R., & Hager, L. P. (1979) *Biochemistry 18*, 2280.

Thomas, J. A., Morris, D. R., & Hager, L. P. (1970) *J. Biol. Chem. 245*, 3129.

Tsubaki, M., & Ichikawa, Y. (1985) *Biochim. Biophys. Acta 827*, 268.

Tsubaki, M., Srivastava, R. B., & Yu, N. T. (1982) *Biochemistry 21*, 1132.

Uno, T., Nishimura, Y., Makino, R., Itzuka, T., Ishimura, Y., & Tsuboi, M. (1985) *J. Biol. Chem. 260*, 2023.

White, R. H. (1981) *Anal. Biochem. 114*, 349.

Yu, N. T., Kerr, E. A., Ward, B., & Chang, C. K. (1983) *Biochemistry 22*, 4534.